Brain Pathology ISSN 1015-6305

RESEARCH ARTICLE

Increased Amoeboid Microglial Density in the Olfactory Bulb of Parkinson's and Alzheimer's Patients

Karlijn J. Doorn[1,2,*]; Andrea Goudriaan[2,*,†]; Carla Blits-Huizinga[2]; John G.J.M. Bol[2]; Annemieke J. Rozemuller[3]; Piet V.J.M. Hoogland[2]; Paul J. Lucassen[1]; Benjamin Drukarch[2]; Wilma D.J. van de Berg[2]; Anne-Marie van Dam[2]

[1] Swammerdam Institute for Life Sciences, Center for Neuroscience, University of Amsterdam, Departments of [2] Anatomy and Neurosciences and [3] Pathology, VU University Medical Center, Neuroscience Campus Amsterdam, Amsterdam, The Netherlands.

Keywords
Alzheimer's disease, anterior olfactory nucleus, hyperphosphorylated tau, microglia, neuroinflammation, olfactory bulb, Parkinson's disease, α-synuclein, β-amyloid.

Corresponding author:
Anne-Marie van Dam, Van der Boechorststraat 7, 1081 BT Amsterdam, The Netherlands (E-mail: *Amw.vandam@vumc.nl*)

Received 23 May 2013
Accepted 12 August 2013
Published Online Article Accepted 23 August 2013

* Both authors contributed equally
† Present address: VU University, Faculty of Earth and Life Sciences, Department of Molecular and Cellular Neurobiology, Amsterdam, The Netherlands

doi:10.1111/bpa.12088

Abstract

The olfactory bulb (OB) is affected early in both Parkinson's (PD) and Alzheimer's disease (AD), evidenced by the presence of disease-specific protein aggregates and an early loss of olfaction. Whereas previous studies showed amoeboid microglia in the classically affected brain regions of PD and AD patients, little was known about such changes in the OB. Using a morphometric approach, a significant increase in amoeboid microglia density within the anterior olfactory nucleus (AON) of AD and PD patients was observed. These amoeboid microglia cells were in close apposition to β-amyloid, hyperphosphorylated tau or α-synuclein deposits, but no uptake of pathological proteins by microglia could be visualized. Subsequent analysis showed (i) no correlation between microglia and α-synuclein (PD), (ii) a positive correlation with β-amyloid (AD), and (iii) a negative correlation with hyperphosphorylated tau (AD). Furthermore, despite the observed pathological alterations in neurite morphology, neuronal loss was not apparent in the AON of both patient groups. Thus, we hypothesize that, in contrast to the classically affected brain regions of AD and PD patients, within the AON rather than neuronal loss, the increased density in amoeboid microglial cells, possibly in combination with neurite pathology, may contribute to functional deficits.

INTRODUCTION

Neuroinflammatory processes have been implicated in the pathogenesis of various neurodegenerative disorders, including Parkinson's (PD) and Alzheimer's disease (AD) (23, 30). Under degenerative conditions, the resting microglial cells, that represent the brain's innate immune system, rapidly transform from morphologically ramified into amoeboid-shaped cells. During this transition, they acquire specific functions like phagocytosis, while they can also secrete cytokines, chemokines, reactive oxygen species (ROS) and growth factors (38, 81). *In vivo* imaging as well as human post-mortem studies have revealed the presence of reactive microglia and proinflammatory mediators at the classical pathological sites in the PD (22, 47, 48, 54) and in the AD brain (55, 78). In post-mortem tissue, microglia with a reactive phenotype accumulate not only around α-synuclein (α-syn) aggregates in the substantia nigra (SN) of PD patients (47), but also around beta amyloid (Aβ) plaques and neurofibrillary tangles (NFT) in the hippocampus (HC) and entorhinal cortex (EC) of AD patients (16, 47, 58, 64). Moreover, polymorphisms in genes encoding various inflammatory cytokines have been associated with a greater risk to develop AD or PD (17, 26).

In vitro application of Aβ, or α-syn, to cultured microglia influences their phagocytic properties, and possibly those of astroglial cells, while increasing their secretion of inflammatory mediators, such as tumor necrosis factor-alpha (TNFα) and ROS (31, 57). Activation of microglia by pathological protein deposits has further been linked to increases in neurotoxicity and degeneration (4, 62, 85) as supported by *in vivo* data from related PD and AD mouse models (72, 73). Taken together, this suggests a putative role for activated microglia and inflammatory mediators in the mechanisms of protein pathology and/or neuronal loss in PD and AD.

Recently, attention has shifted away from the SN in PD, or the HC and EC in AD patients as the only pathological sites, to other affected brain regions. This shift was further encouraged by histopathological studies indicating that α-syn pathology in PD, and the NFTs and Aβ plaques in AD, spread throughout the brain in a well-defined anatomical sequence (6, 8). Further evidence for a "prion-like" hypothesis for α-syn spreading and a causal relationship with neuronal death was recently provided by a study showing cell-to-cell transmission of pathological α-syn in wild-type mice after a single intracerebral injection of synthetic α-syn fibrils (45). In PD, α-syn pathology in the olfactory bulb (OB) is an early event and present already during presymptomatic stages

of the disease (7). The occurrence of NFTs in the OB of AD patients further seems to reflect early neuropathology as well, as it occurs in advance of, or in parallel to, the Aβ pathology in the EC (2, 37, 75).

Interestingly, in both PD and AD, neuropathology in the OB appears concentrated in the anterior olfactory nucleus (AON) mostly, a dispersed region within the granular cell layer of the OB and olfactory tract that is important for olfactory function (11, 43). Notably, these neuropathological changes are consistent with the characteristic olfactory impairments in *de novo* PD patients as well as hyposmia as an early symptom in AD (15, 19, 27, 60). Moreover, olfactory dysfunction seems to relate to disease progression in both the pre-motor and motor phase of PD (3, 51).

Previously, we observed microgliosis and elevated expression of interleukin-1 family members in the OB of 1-methyl-4-phenyl-1,2,3,6-tetrahydropyridinel (MPTP)-treated mice, supporting that in this animal model for PD, neuroinflammatory responses extend beyond the nigrostriatal areas (80). In the present study, we focus on the activational status of microglial cells in the human OB and their relationship with protein pathology or neuronal degeneration. Therefore, we assessed densities of amoeboid microglial cells, ramified microglial cells and neurons in the AON by using a morphometric approach in well-characterized cohorts of AD and PD patients and control subjects, while neurite pathology was also investigated. Subsequently, correlations between pathological protein levels and the densities of amoeboid microglia were examined and we carefully studied colocalization of pathological protein aggregates and microglia or astrocytes, as an indicator for possible phagocytosis and local clearance of pathological protein deposits within the AON.

MATERIALS AND METHODS

Human subjects

Human post-mortem brain tissue was obtained from the Netherlands Brain Bank (NBB, Amsterdam, The Netherlands) or from the Department of Pathology, VU University Medical Center in Amsterdam, The Netherlands. In compliance with all local ethical and legal guidelines, all donors had given written informed consent for brain autopsy, for use of brain tissue and for allowing access to the neuropathological and clinical information for scientific research. The OB and ventral mesencephalon were included from seven clinically diagnosed and neuropathologically verified PD patients as well as the OB and HC from eight patients with clinically diagnosed and neuropathologically verified AD. The control group consisted of 11 subjects without neurological or psychiatric disease, of which all above mentioned brain regions were studied. The age of the PD patients ranged from 73 to 88 years, the age of the AD patients ranged from 62 to 86 years and the control subjects ranged from 66 to 93 years of age. The clinicopathological data, including cause of death and Braak staging for PD and AD of all donors are summarized in Table 1.

Tissue processing

After autopsy, brain regions were dissected and immersion-fixed in 4% formaldehyde for 4 weeks, after which they were embedded in paraffin. From the paraffin blocks that contained the ventral mesencephalon, which included the SN pars compacta and from the HC, 6 μm sections were cut on a microtome and dried in an oven overnight at 37°C before immunohistochemical analysis. From the entire OB, 20 μm horizontal sections were cut and dried, and every 10th section was used for immunohistochemical staining and morphometric analysis. Sections were mounted on positively charged glass slides (Menzel-Glaser SuperFrost plus, Braunschweig, Germany).

Immunohistochemistry

Sections were heated in a stove for 1 h at 56°C, before they were deparaffinized and rehydrated through a graded series of ethanol. For subsequent antigen retrieval, sections were rinsed in 0.01 M citrate buffer (pH 6.0) or in 10 mM Tris buffer (pH 9.0) containing 1 mM EDTA (Tris-EDTA) and afterwards placed in preheated citrate buffer or Tris-EDTA, respectively in a steamer for 30 minutes at 90–99°C. For α-syn staining, antigen retrieval was performed using pretreatment with 100% formic acid for 10 minutes. After pretreatment, the sections were allowed to regain room temperature (RT), rinsed in Tris-buffered saline (TBS), and incubated for 20 minutes in TBS containing 0.3% H_2O_2 and 0.1% sodiumazide. Non-specific binding sites were blocked with 5% non-fat dried milk in TBS containing 0.5% Triton (TBS-T; blocking solution) for 30 minutes at RT. Subsequently, sections were incubated overnight at 4°C with mouse anti-CD68, mouse anti-Aβ, mouse anti-α-syn, or mouse anti-hyperphosphorylated tau (HPtau) antibodies (see Table 2 for details on primary antibodies), diluted in blocking solution. Following this, sections were washed in TBS and incubated for 2 h at RT in biotinylated donkey anti-mouse IgG's (1:400, Jackson Immunoresearch, Westgrove, PA, USA), followed by HRP-labeled avidin-biotin complex (ABC complex 1:400; Vector Laboratories, Burlingame, CA, USA) for 1 h at RT. Staining was visualized using 3,3-diaminobenzidine (DAB, Sigma, St. Louis, MO, USA) as chromogen and counterstaining was performed with Nissl. After dehydration in graded ethanol solutions, the sections were cleared in xylene and coverslipped in Entellan (Merck, Darmstadt, Germany).

Bodian silver staining

To examine possible neuropathological changes in the neurites and general anatomy of the neuronal network, a classic Bodian silver staining protocol was used (5). The silver solution (2 g albumin silver in 200 mL H_2O) was applied overnight at 37°C to deparaffinized and rehydrated sections of the OB with copper sheets. Sections were washed in H_2O and subsequently treated for 10 minutes with hydroquinone (2 g in 10 mL 37% formaldehyde and 200 mL H_2O). Sections were again washed in H_2O. To increase contrast, a 1% gold-chloride solution was applied for 2–5 minutes. Thereafter, the sections were washed with H_2O and incubated with 1.5% oxalic acid in H_20 for 5 minutes. Surplus silver was removed with 5% sodium thiosulfate in H_2O (5–10 minutes). Sections were dehydrated in graded ethanol solutions, cleared in xylene and coverslipped in Entellan (25).

Immunofluorescence

For double-labeling of glial cells and pathological proteins, a combination of antibodies for microglia, that is, CD68, or

Table 1. Patient information. Abbreviations: AD = Alzheimer's disease; C = control subject; D = clinical and neuropathological diagnosis; NFT = neurofibrillary tangles; PD = Parkinson's disease; PMD = post mortem delay.

Patient number	D	Gender	Age	PMD (h)	Brain weight (g)	Braak α-synuclein stage	Braak NFT stage	Braak amyloid stage	Cause of death
1	C	M	74	5:00	1125	0	3	C	Brochus carcinoma
2	C	M	80	7:15	1376	0	0	0	Cachexia and dehydration
3	C	M	91	8:00	1243	1	1	B	Cardiac decompensation
4	C	F	93	5:50	1145	0	2	0	Mamma carcinoma
5	C	F	93	4:25	1223	0	1	A	Unknown
6	C	F	85	5:00	1257	0	1	B	Ruptured abdominal aneurysm
7	C	F	85	4:40	1168	1	2	A	Dehydration
8	C	M	66	7:45	1590	0	0	0	Ruptured abdominal aneurysm aorta
9	C	F	84	4:45	1179	0	1	0	Heart failure
10	C	F	89	6:25	1210	0	2	B	Old age
11	C	M	84	5:35	1457	0	1	A	Heart failure
12	PD	M	88	5:50	1205	6	1	C	Unknown
13	PD	F	87	5:25	1195	6	2	B	Pneumonia
14	PD	M	84	6:05	1243	5	1	C	Myocardial infarction
15	PD	M	73	6:35	1572	3	1	A	Aspiration pneumonia
16	PD	F	84	7:25	1244	5	2	B	Unknown
17	PD	M	87	3:40	1205	5	1	B	Cachexia and dehydration
18	PD	M	80	7:05	1612	6	1	B	Pneumonia
19	AD	M	67	4:10	1387	0	5	C	Cachexia
20	AD	M	64	11:16	1066	0	6	C	Cachexia and dehydration
21	AD	F	86	5:55	950	0	4	B	Cachexia
22	AD	M	62	6:45	1011	0	6	C	Aspiration pneumonia
23	AD	F	83	4:55	1250	0	6	C	Dehydration
24	AD	F	84	4:50	1120	0	4	C	Cardiac arrest
25	AD	F	77	6:05	1059	0	5	C	Pneumonia
26	AD	F	73	5:55	1090	0	6	C	Unknown

astrocytes, that is, glial fibrillary acidic protein (GFAP), and for Aβ, HPtau, or α-syn were used. Sections were sequentially incubated (CD68/HPtau, CD68/Aβ) or co-incubated (CD68/α-syn, GFAP/HPtau, GFAP/Aβ, GFAP/α-syn) with the appropriate primary antibodies. Co-incubations of sections with anti-α-syn and anti-CD68 were pretreated with Tris-EDTA (pH 9.0). Sections to be stained for all other antibody combinations were pretreated with citrate buffer (pH 6.0). All antibodies were diluted in the blocking solution as indicated above. After a 48 h incubation at 4°C, the sections were washed and subsequently incubated for 90 minutes at RT with appropriate Alexa Fluor 488 or Alexa Fluor labeled 594 IgG's or with streptavidin-labeled Alexa Fluor 594 (1:400, Jackson Immunoresearch) when the primary antibodies were already biotinylated (see Table 3 for detailed information on primary antibodies and conjugates). After washing, the sections were coverslipped with Vectashield (Vector Laboratories, Burlingame, CA, U.S.A.). Sections were examined using a confocal laser scanning microscope (Leica TSC-SP2-AOBS; Leica Microsystems, Wetzlar, Germany).

Delineation of the AON for quantification of microglial and neuronal cell numbers

The OB was identified by the presence of the glomerular cell layer; the AON was recognized as a clearly demarcated group of medium-to-large sized pyramidal neurons with a diameter of 15–20 μm in the granular cell layer of the OB in the Nissl-stained horizontal sections (11, 43). AON parts that extended into the olfactory tracts and substantia perforata anterior were rare and excluded from analysis. Delineation of the total AON was performed in each section by outlining the separate groups of large neurons that were just slightly Nissl-positive (Figure 1A, B).

Table 2. Primary antibodies used for single labeling.

Antigen	Species	Final dilution	Source
Human CD68	Mouse	1:400	DAKO, clone KP1
Human hyperphosphorylated Tau	Mouse	1:1000	Innogenetics, clone AT-8
Human β-amyloid	Mouse	1:500	DAKO, MO872
Human α-synuclein	Mouse	1:2000	BD-Bioscience, 610 786
Cow GFAP	Rabbit	1:2000	DAKO, ZO334

Table 3. Antibodies (ab's) and conjugates used for double labeling.

Antigen	Species	Final dilution	Source	Secondary ab's and conjugates
Human CD68	Mouse	1:300	DAKO, clone KP1	DoaM-AF488 1:400
Human α-synuclein	Goat	1:200	Santa Cruz sc 7012	DoaG-AF594 1:400
Cow GFAP	Rabbit	1:2000	DAKO, ZO334 +	DoaR-AF594 1:400
Human α-synuclein	Goat	1:200	Santa Cruz sc 7012	DoaG-AF488 1:400
Human CD68	Mouse	1:300	DAKO, clone KP1	DoaM-AF488 1:400
Biotinylated human hyperphosphorylated Tau	Mouse	1:100	Thermo Scientific	Streptavidin-AF594
Cow GFAP	Rabbit	1:2000	DAKO	DoaR-AF488 1:400
Human hyperphosphorylated tau	Mouse	1:300	Innogenetics	DoaM-AF594 1:400
Human CD68	Mouse	1:300	DAKO, clone KP1	DoaM-AF488 1:400
Biotinylated human β-amyloid	Mouse	1:400	Covance, SIG39240	Streptavidin-AF594
Cow GFAP	Rabbit	1:2000	DAKO, ZO334	DoaR-AF594 1:400
Human β-amyloid	Mouse	1:1000	Chemicon mab1561	DoaM-AF488 1:400

Identification criteria of ramified and amoeboid microglia, and of AON neurons

Microglial cells were identified by positive CD68-immunoreactivity (32). While both microglial subtypes are characterized by a cytoplasmic staining, the ramified microglial cell type can be clearly distinguished as it has a small cell body and thin, radially projecting processes (Figure 1C). The amoeboid type of microglia is characterized by a densely CD68-stained cell body typically surrounded by no or only very few short/stump processes (Figure 1D). CD68-immunopositive cells wrapped around or touching blood vessels were not included to avoid overlap with blood-derived monocytes. AON neurons were identified by their large size with little Nissl substance in their cytoplasm (41) and a

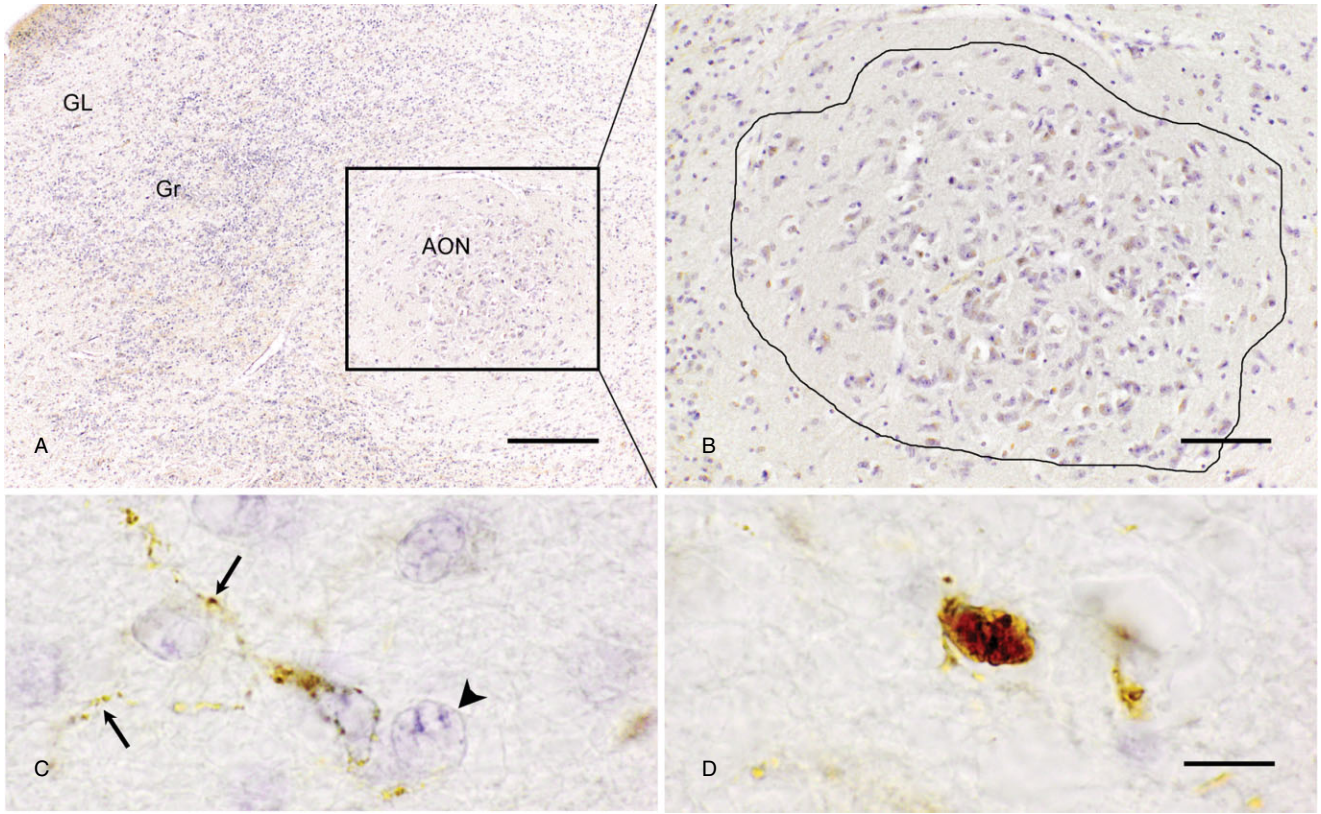

Figure 1. *Delineation of the anterior olfactory nucleus (AON) and cell morphologies to be quantified.* **A.** The AON (square) lies within the granular layer (Gr) of the OB; bar = 250 μm. **B.** Higher magnification of an AON, consisting of large, light Nissl positive, neurons. Line represents the delineation of an AON used for quantification of cells; bar = 100 μm. **C.** Ramified CD68-positive microglial cell showing thin and radially projecting processes (arrows), AON neuron is identified by having a light Nissl stained cytoplasm and a clearly Nissle positive nucleolus (arrowhead). **D.** Amoeboid CD68 positive microglial cells showing a rounded morphology; bar (**C,D**) = 10 μm.

big nucleus containing Nissl substance bound to nucleic acids (Figure 1C).

Quantitative analysis of microglial cells and neurons in the AON using a morphometric approach

Quantitative analysis of the density of microglial cells and neurons within the AON was performed using a computer-assisted morphometry system, consisting of a Leica DMR Axioplan photomicroscope with a CCD color video camera (Optronics, 1200–1660 pixels, Goleta, CA, U.S.A.) and a LEP XY motorized stage with StereoInvestigator software version 9.0 (MicroBrightfield Inc., Colchester, VT, USA). The depth of the focal plane was measured with a Heidenhain MT12 microcator attached to the stage with a resolution of approximately 0.5 μm.

To prevent experimenter bias, all OB sections to be analyzed were coded. The AON was delineated at a final magnification of 100× in sections collected serially throughout the OB, yielding three to six sections in which the AON was visible per subject. The total number of ramified microglia, amoeboid microglia or neurons within the volume fraction of the AON examined was estimated using the optical fractionator (83) workflow of the StereoInvestigator software. As the anatomy of the AON can vary within and between subjects, quantification of the density of microglial cells and neurons in the entire AON of the OB thus needs to be standardized carefully. We therefore counted and subsequently calculated the density of microglial cells and neurons within the volume fraction of the AON examined in the OB ($Volume_{AON}$) using the following equation: cell density = (ΣQ-*(1/tsf)*(1/asf))/$Volume_{AON}$, where ΣQ- is the number of cells counted in the 3D counting frames, asf is the area sampling fraction (counting frame area = 5625 μm^2/grid size area = 8100 μm^2, asf = 0.69). Tsf is the thickness sampling fraction, determined by ratio of the height of the optical dissector probe (ie, 10 μm) and the mean weighted thickness of the sections [13.9 μm, standard error of the mean (SEM) 0.4 μm] included in the analysis. Quantification of the microglial cells and neurons was performed using a 40× objective lens resulting in a final magnification of 400×.

Assessment of AD and PD neuropathology in the AON

The presence and severity of HPtau-immunoreactive NFTs, Aβ-immunoreactive senile plaques and α-syn-immunoreactive Lewy bodies/neurites (LBs/LNs) were analyzed by two trained investigators unaware of the Braak pathological score of each patient. A semi-quantitative scoring of pathology in the AON was performed using a 200 × magnification. A final score ranging from 0 to 4 was assigned to the major histological signatures of AD and PD, as previously done by others (35, 59) with a score of 0 given to the AON devoid of HPtau positive NFTs, Aβ positive senile plaques or α-syn positive LBs/LNs, a score of 1 was given to sparse pathology in the AON. A score of 2 corresponded to moderate deposition and a score of 3 to widespread depositions in the AON. Finally, a score of 4 indicated severe deposition of HPtau positive NFTs, extensive numbers of Aβ positive senile plaques or α-syn positive LBs/LNs in the AON (see Table 4 for pathology score per case).

Table 4. Pathology scores in AON of (1) PD patients and (2) AD patients. Abbreviations: AD = Alzheimer's disease; NFT = neurofibrillary tangles; n.a = not available; PD = Parkinson's disease.

(1)				
Patient number	Diagnosis	α-synuclein score	NFT score	β-amyloid score
12	PD	1	1	3
13	PD	2	3	n.a
14	PD	3	2	n.a
15	PD	1	1	0
16	PD	3	1	0
17	PD	3	1	3
18	PD	2	1	n.a
(2)				
Patient number	Diagnosis	β-amyloid score	NFT score	α-synuclein score
19	AD	1	4	1
20	AD	3	4	3
21	AD	2	2	0
22	AD	4	3	0
23	AD	3	2	1
24	AD	2	2	0
25	AD	1	4	0
26	AD	0	4	0

Statistical analysis

The mean and SEM of microglial and neuron densities in the OB were calculated for each patient group. Normal distribution of the data was demonstrated by Kolmogorov–Smirnov significance tests. When normal distributions were not apparent, analysis was performed on log10 transformed data. For the cell density calculations, stepwise multiple regression analyses were performed to control for possible influences of age, gender, post-mortem delay (PMD) and whole brain weight. Amoeboid microglia density showed an inverse correlation with overall brain weight ($r = -0.65$, $P = 0.001$). Therefore, this variable was taken as covariate in the subsequent one-way independent multivariate analysis of covariance (MANCOVA), performed for amoeboid microglial density, ramified microglial density and neuronal density. The main analysis was followed up by Bonferroni corrected, pairwise comparisons. Correlation analysis was performed using Spearman rank correlation analysis. Statistical analyses were performed with the SPPS package version 20.0 (Statistical Product and Service Solutions, Chicago, IL, USA).

RESULTS

Microglial phenotypes in classical pathological brain regions of AD and PD patients

Before studying microglial cell morphology in the OB, we examined microglial phenotypes in the SN of PD patients and in the HC of AD patients as activated microglial cells were reported to be present in these brain regions (47, 55). In the SN of control subjects, numerous neuromelanin-pigmented, dopaminergic neurons

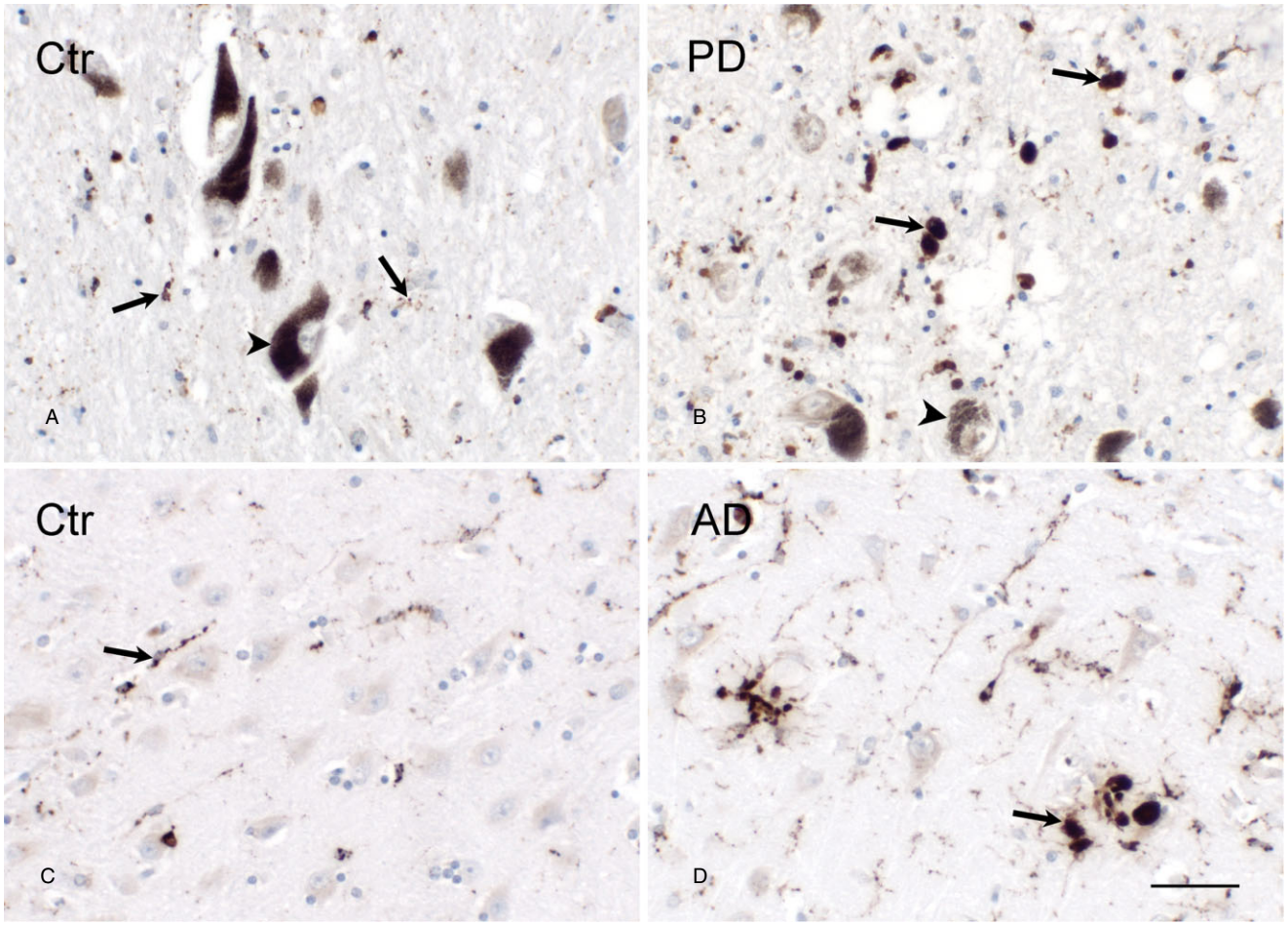

Figure 2. *Appearance of amoeboid microglia in the SN of PD patients and in the HC of AD patients.* **A.** Representative image of the SN of a control subject. Neuromelanin pigmented neurons were recognized by a dark coloring around large neuronal nuclei (arrowhead). CD68 positive ramified microglia (arrow) were observed randomly within the SN. **B.** Representative image of the SN of a PD patient. Degraded neuromelanin pigmented neurons were present in the SN (arrowhead). CD68 positive amoeboid microglia (arrow) appeared at the degenerative site. **C.** Representative image of CD68 immunoreactivity in the Ammon's horn of a control subject. CD68 positive ramified microglia (arrow) were detected. **D.** Representative image of the Ammon's horn of an AD patient. Numerous clustered CD68 positive amoeboid microglia (arrow) appeared; bar (**A–D**) = 50 μm.

were recognized by a dark discoloration around large neuronal nuclei while CD68-positive microglia had long and fine processes, indicative of their ramified state (Figure 2A). In contrast, PD patients showed an extensive loss of neuromelanin-containing, dopaminergic neurons in the SN (Figure 2B). Moreover, there was an increased appearance of CD68-positive amoeboid microglia, the phenotype associated with microglial activation (Figure 2B). In the Ammon's horn of the HC of AD patients, similar results were obtained. Numerous and widespread microglial cells with ramified morphology were detected in control subjects, whereas in AD patients, additional clusters of amoeboid cells were seen, frequently localized around Aβ plaques (Figure 2C, D, respectively).

HPtau-, Aβ and α-syn pathology in the OB

The presence of disease-specific proteopathy was subsequently determined in the OB of PD and AD patients. Aberrant α-syn (Figure 3A), Aβ (Figure 3C) and HPtau (Figure 3E) immunoreactivity were less present or absent in the AON of control subjects. In contrast, α-syn staining was prominent in the AON of PD patients (Figure 3B), whereas in AD patients, Aβ and HPtau protein was abundantly expressed in the AON (Figure 3D, F, respectively). Furthermore, only a few AD and PD patients presented some α-syn or Aβ pathology in the AON, respectively, whereas all PD patients showed HPtau pathology, although to a lesser extent than in AD patients.

Microglial phenotypes in the AON

In the OB of control subjects and of PD and AD patients, CD68 positive microglia with a ramified morphology were present in various layers of the OB, and also in the AON (Figure 4A–C). In control subjects, the presence of amoeboid microglia was less prominent (Figure 4A) when compared to the increased

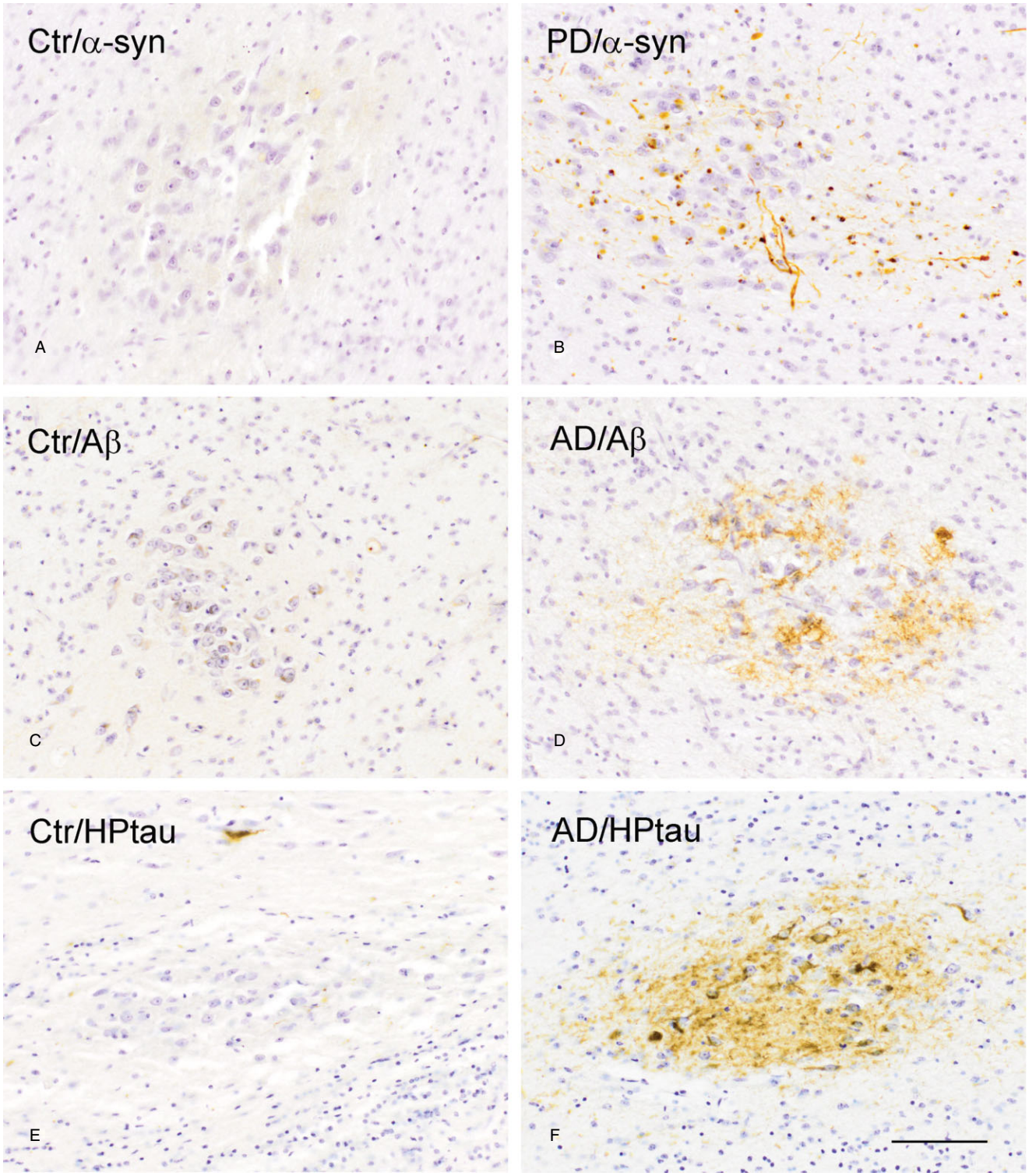

Figure 3. *Protein pathology in the AON of control subjects, PD and AD patients.* (**A**) α-syn, (**C**) Aβ and (**E**) HPtau immunoreactivity in the AON of control subjects is minimal compared to (**B**) α-syn immunoreactivity in the AON of PD patients, and (**D**) Aβ and (**F**) HPtau immunoreactivity in the AON of AD patients; bar (**A–F**) = 100 μm.

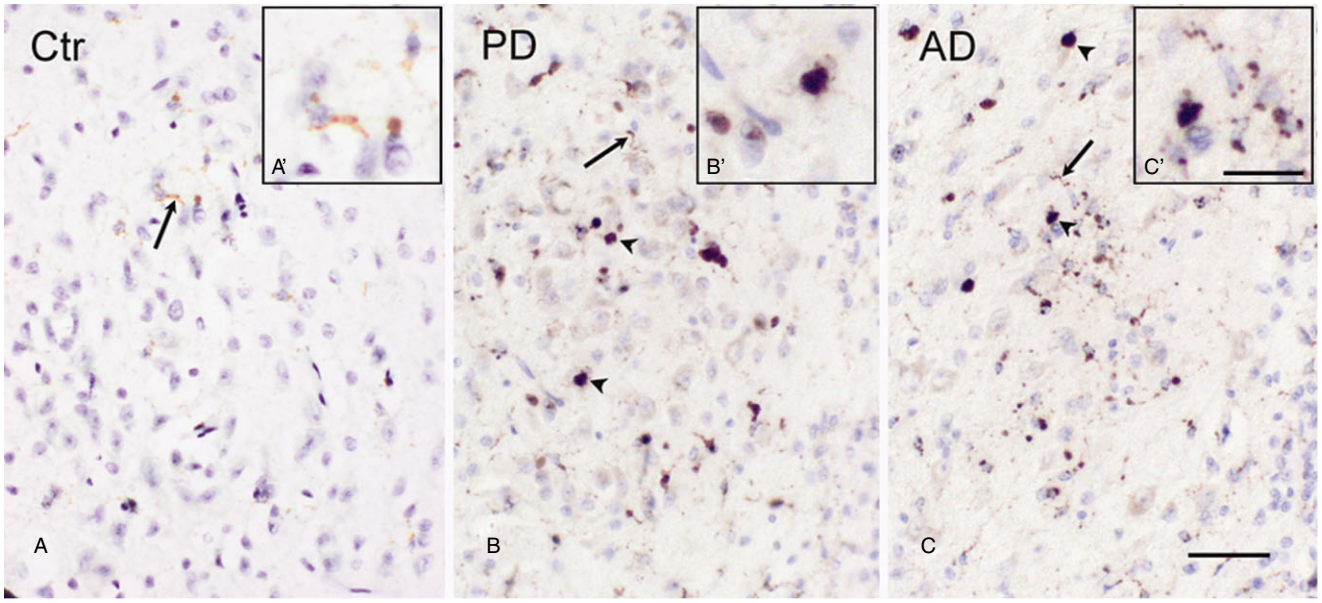

Figure 4. *CD68 immunoreactivity in the AON of control subjects, PD patients and AD patients.* **A.** a control subject showing CD-68 positive ramified microglial cells (arrow), (**A'**) magnification of ramified microglial cells. **B.** A PD patient showing CD-68 positive ramified (arrow) and amoeboid (arrowhead) microglial phenotypes, (**B'**) magnification of amoeboid microglial cell. **C.** An AD patient, showing CD-68 positive ramified (arrow) and amoeboid (arrowhead) microglial phenotypes, (**C'**) magnification of amoeboid and ramified microglial cells; bar (**A–C**) = 50 μm, bar (**A'–C'**) = 25 μm.

appearance of microglia with an amoeboid morphology within the AON of PD (Figure 4B) and AD patients (Figure 4C) which was a consistent finding.

Quantitative analysis of microglial cells and neurons in the AON

We used an unbiased random systematic sampling method to examine microglial and neuron densities in the AON of control subjects, PD and AD patients. Age, gender and PMD had no influence on any of the densities examined. The multivariate results of the MANCOVA indicated a significant effect of brain weight covariate ($F(3,20) = 4.76$, $P = 0.012$). Nonetheless, a main effect for group was reported as well ($F(6,38) = 4.04$, $P = 0.003$). Subsequent univariate analysis revealed that a group effect was only significant for the number of amoeboid microglial cells per mm^3 ($F(2,22) = 10.86$, $P = 0.001$; mean control subjects $6.65 \times 10^3 \pm 1.61$, mean PD patients $25.54 \times 10^3 \pm 7.05$, mean AD patients $39.26 \times 10^3 \pm 6.75$). No significant differences were apparent for the number of ramified microglia per mm^3 ($F(2,22) = 1.89$, $P = 0.174$; mean control subjects $28.79 \times 10^3 \pm 2.67$, mean PD patients $24.04 \times 10^3 \pm 4.91$, mean AD patients $19.42 \times 10^3 \pm 2.79$). For the number of neurons per mm^3, statistical significance was also not reached ($F(2,22) = 2.01$, $P = 0.157$; mean control subjects $72.06 \times 10^3 \pm 4.82$, mean PD patients $66.79 \times 10^3 \pm 5.19$, mean AD patients $61.28 \times 10^3 \pm 4.16$). Compared to control subjects, increases in the density of amoeboid microglia were significant for both PD ($P = 0.002$) and AD patients ($P = 0.003$). These differences were quite prominent, with approximately four- to sixfold increases in amoeboid microglia densities for PD and AD patients, respectively (Figure 5).

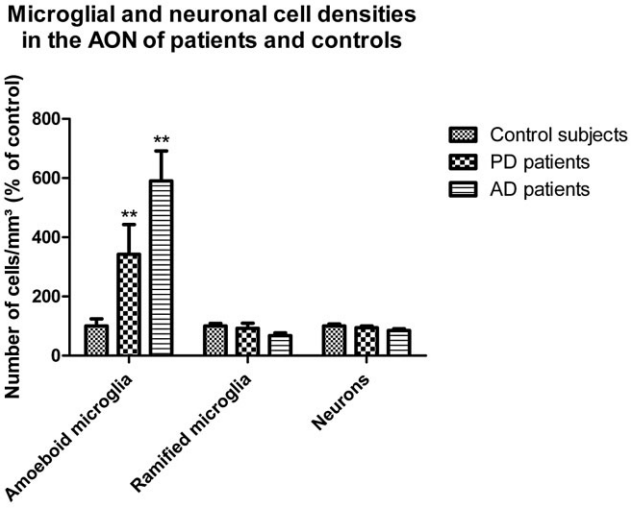

Figure 5. *Quantification of cell densities within in the AON of control subjects, PD and AD patients.* Quantification by a morphometric approach resulted in significant enhance densities of amoeboid microglia in the AON of PD and AD patients compared to control subjects ($P = 0.002$, $P = 0.003$, respectively). The densities of ramified microglia and neurons within the AON were not different between control subjects and PD or AD patients. Data represent mean ± SEM, $^{**}P < 0.01$ (vs. control subjects).

Correlation between amoeboid microglia density and protein pathology scores in the AON

The local protein pathology in the AON of the patient groups was scored semi-quantitatively (Table 4). These scores were correlated to the amoeboid microglia densities within the respective patient group. Aβ immunoreactivity scores in the AON of AD patients correlated positively with the density of amoeboid microglia (rho = 0.764, n = 8, $P = 0.027$*). Interestingly, HPtau immunoreactivity within the AON of AD patients showed a significant negative correlation with the density of amoeboid microglia (rho = −0.756, n = 8, $P = 0.03$*). We also correlated α-syn pathology scores with amoeboid microglia within AD patients and found no correlation [rho = −0.261, n = 8, $P = 0.053$ not significant (NS)]. Within PD patients, α-syn immunoreactivity scores in the AON showed no significant correlation with the density of amoeboid microglia (rho = 0.170, n = 7, $P = 0.715$ NS). HPtau and Aβ immunoreactivity scores within PD patients were taken into account but showed no correlation with amoeboid microglia (rho = 0.178, n = 7, $P = 0.702$ NS and rho = 0.894, n = 4, $P = 0.106$ NS, respectively)

No colocalization of CD68 or GFAP with pathological proteins

The presence of amoeboid microglia near pathological protein aggregates might reflect a role in phagocytosis of aberrant proteins. Using confocal microscopy, CD68 immunopositive microglia with an amoeboid morphology were found to surround α-syn aggregates in the AON (Figure 6A) and SN (Figure 6B) of PD patients as well as Aβ and HPtau in the AON (Figure 6C, E, respectively) and HC (Figure 6D, F, respectively) of AD patients. Based upon these double-labeling studies, neither colocalization between Aβ or HPtau and CD68 positive amoeboid microglia was observed in the AON of AD patients, nor did α-syn colocalize with CD68 in PD patients. Similarly, colabeling with GFAP showed that the pathological proteins in the AON (Figure 7A) and SN (Figure 7B) of PD patients, and in the AON (Figure 7C, E) and HC (Figure 7D, F) of AD patients, were not colocalized with astrocytes.

Neurites in the AON

Within the AON, Bodian silver staining revealed normal appearing neurites in control subjects (Figure 8A) whereas in the AON of the AD and PD patients, a typical pathological pattern was found with morphologically altered neurites (Figure 8B, C).

DISCUSSION

In the present study, we show the presence of amoeboid and ramified microglia phenotypes in the OB of PD and AD patients, a non-traditional pathological site, which is affected early in both disorders. While a significant increase was found in the densities of amoeboid microglia in the AON in both disorders, indicative of an activated state of the cells, the absence of colocalization with pathological protein aggregates indicates that microglia in the AON do not exert extensive phagocytic activity toward these disease-specific protein deposits. Although neurites appeared morphologically different in PD and AD patients, this was not paralleled by overt neuronal loss in the AON.

The accumulation of disease-specific proteins in the AON of our verified PD and AD patient cohorts is consistent with previous studies demonstrating the presence of Aβ plaques and NFTs in the OB of AD patients, and of α-syn inclusions in the OB of PD patients (8, 9, 50, 63, 75). The localization of these pathological proteins mainly within the AON suggests a selective vulnerability of this region that is functionally involved in the processing of olfactory information (61).

Neuroinflammatory processes, including microglial activation, have consistently been shown to play a role in neurodegeneration. While microgliosis had been observed in the OB of MPTP-treated mice (37, 75, 80), it was still unknown whether microglial cells within the OB were altered in the human disorder as well, and which phenotypes were involved. Our state-of-the-art quantification revealed a substantial and specific increase in amoeboid microglial density, suggesting that these cells are activated in the AON of PD and AD patients. As similar observations have been made in another non-traditional pathological site in PD, the hippocampus (34), microglial activation may not be solely occurring in the nigrostriatal region, but may rather arise at several pathological sites in PD. Moreover, the density of amoeboid microglial cells in the AON of PD patients did not correlate with the extent of α-syn pathology, suggesting that the increased microglial activation in this region is not proportional to the extent of α-syn deposition, but rather that a local presence of α-syn pathology is already sufficient to evoke microgliosis (71). Within other brain regions, this may be different (82) as in the SN of PD patients a positive correlation has been found before between microglial cell activation and α-syn deposition (12). Hence, microglia may respond differentially to α-syn pathology in the AON compared to the SN of PD patients because of differences in microglial cell subtypes (18, 24). The concomitant differences in local environment may have various consequences for neuronal functioning (18).

In AD patients, a significant positive correlation was observed between the density of amoeboid microglial cells and the level of Aβ deposits in the AON. These observations are in line with previous correlations reported between microglial activation and the severity of Aβ deposition in the HC (77). Unexpectedly, HPtau levels and amoeboid microglia density in the AON of AD patients showed a significant negative correlation. The level of HPtau was, at least in most of the individual AD patients, inversely related to the level of Aβ scores within the AON of the same patient. This "within patient effect" could explain the negative correlation between HPtau and amoeboid microglia.

The lack of a positive correlation between α-syn or HPtau deposition and amoeboid microglial densities within the AON of PD or AD patients, respectively, suggests that irrespective of the level of these pathological proteins, microglial cells are affected, and become activated. This does not seem to hold for Aβ deposition that does correlate with amoeboid microglial density, and may be explained by the fact that Aβ is deposited outside the cell, and could thus act as a "dose-dependent" stimulus for microglial activation, whereas α-syn and HPtau are mostly intracellularly deposited (13, 65, 66), but can be externalized to have paracrine effects (28, 42), for example, activate local microglial cells.

Since a common hypothesis focuses on a predominantly detrimental role of activated microglia, we quantified the number of

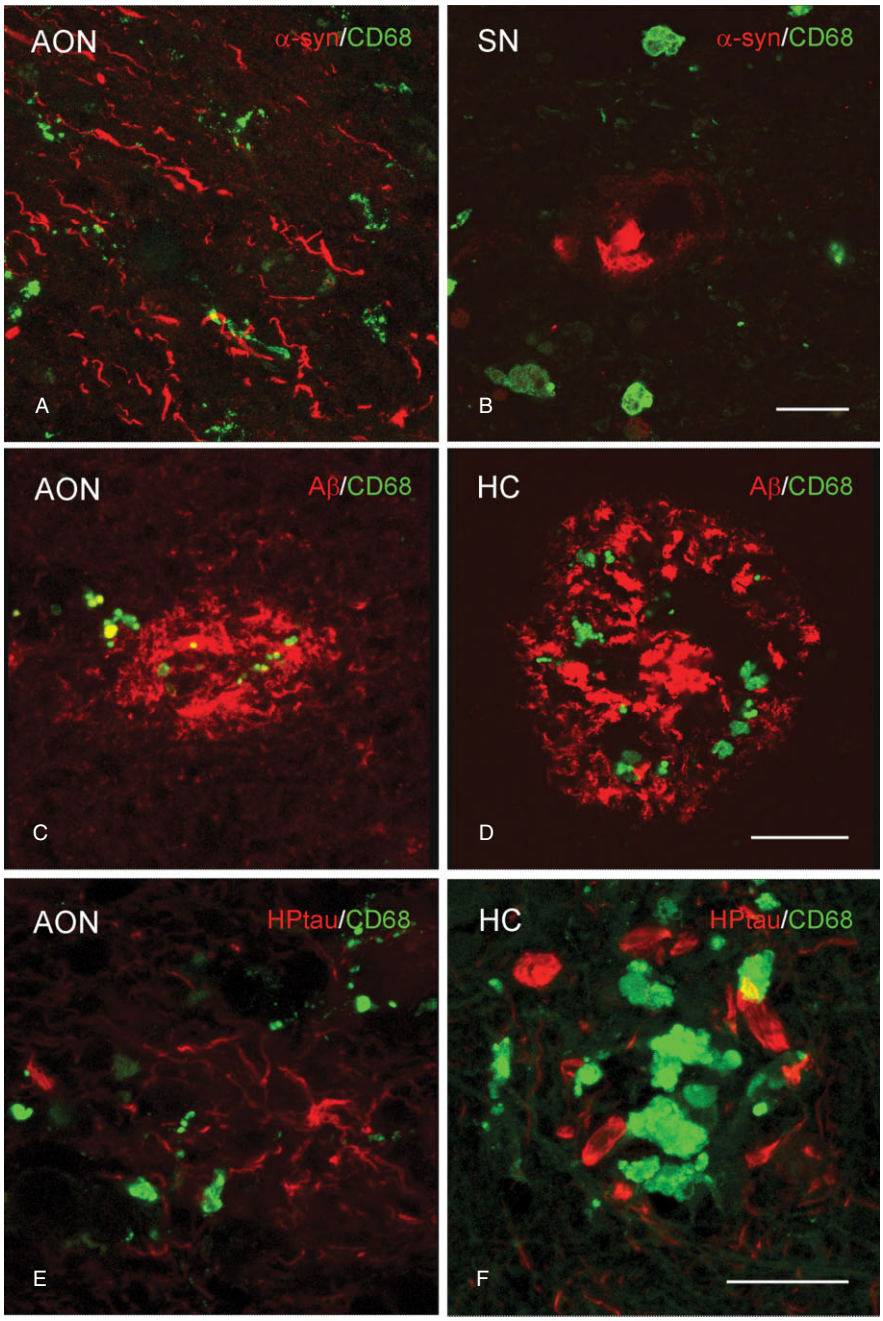

Figure 6. *Absence of colocalization of CD68 positive microglia and protein aggregates in PD and AD patients.* Representative images of confocal laser scanning microscopy revealed (**A,B**) no colocalization of CD68 (green) with α-syn (red) in the (**A**) AON or (**B**) SN of PD patients. **C,D.** In AD patients, CD68 (green) colocalized with Aβ (red) in the (**C**) AON but not in the (**D**) HC. **E,F.** In AD patients no colocalization of CD68 (green) with HPtau (red) in the (**E**) AON or (**F**) HC was found; bar (**A–F**) = 20 μm.

Nissl-positive neurons within the AON but no differences were observed in the densities of large AON neurons between PD patients, AD patients and control subjects. In contrast to the extensive neurodegeneration in the SN of PD and HC of AD patients, our present data indicate that activated microglial cells in the AON are not related to any local neuronal loss. Although we cannot exclude a limited vulnerability of AON neurons (10), it is worth noting that the OB is part of the neurogenic pathway (14) and new-born neurons residing in the OB might, at least in theory, compensate for PD and AD related neuronal degeneration (39, 46, 76). Moreover, the number of dopaminergic neurons is increased in the glomerular layer of the OB of PD patients, indeed suggesting that some compensatory mechanisms may occur in the AON (33, 50). As the Bodian silver staining did reveal a typical neuropathological pattern with altered neurite morphology, indicative of dystrophic neurites (5, 53) within the AON of these patients, it is tempting to speculate that these structural changes may affect AON functionality and could contribute to the olfactory deficits in PD and AD patients. This notion agrees with more general concepts proposing that network dysfunction rather than neuronal death per se, likely underlies several of the clinical manifestations in neurodegenerative diseases, including the cognitive decline in AD (49, 56). On the other hand, HPtau, Aβ and α-syn deposits in the olfactory bulb can affect normal

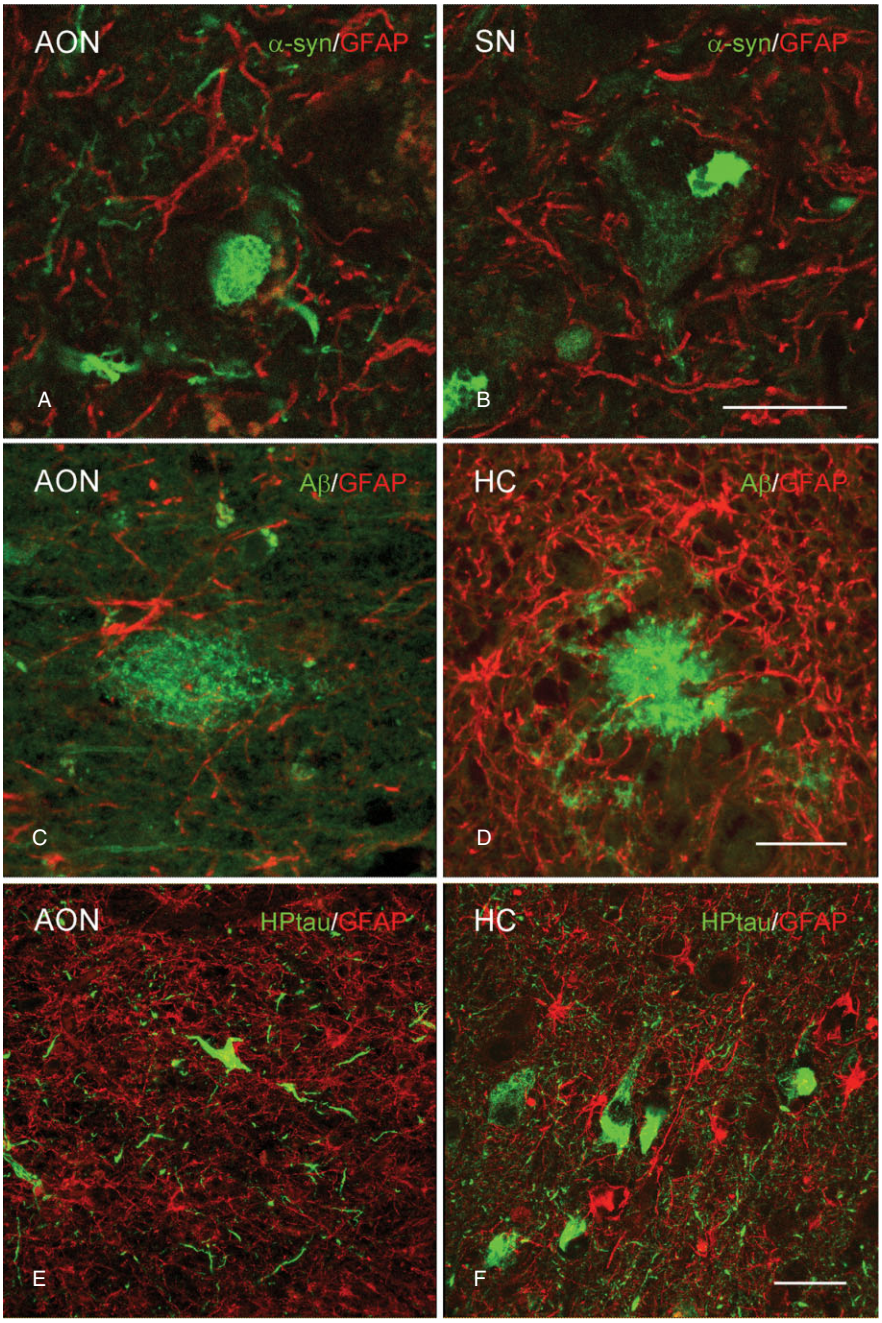

Figure 7. *Absence of colocalization of GFAP positive astrocytes and protein aggregates in PD and AD patients.* Representative images of confocal laser scanning microscopy revealed (**A,B**) no colocalization of GFAP (red) with α-syn (green) in the (**A**) AON or (**B**) SN of PD patients. **C,D.** In AD patients, GFAP (red) did not colocalize with Aβ (green) in the (**C**) AON or (**D**) HC. **E,F.** In AD patients no colocalization of GFAP (red) and HPtau (green) in the (**E**) AON or (**F**) HC was observed; bar (**A–D**) = 20 μm, bar (**E–F**) = 40 μm.

neurotransmitter release and hence cause disturbances in local information processing (50).

We also investigated whether amoeboid microglial cells are engaged in phagocytosis in the AON and SN of PD patients, and in the AON and HC of AD patients. Microglia are commonly seen as scavengers of the central nervous system (CNS), given their enhanced phagocytic properties upon activation *in vitro* (79). Indeed, several *in vitro* studies have presented evidence of phagocytosis of PD or AD related pathological proteins by microglial cells (29, 70). However, few studies have focused on pathological protein phagocytosis by microglia in post-mortem PD or AD tissue. In our study, we could not observe clear immunohistochemical colocalization of microglia with pathological proteins in several affected brain regions. Although the interpretation of such data should be done with care, it suggests that microglia either do not readily phagocytose pathological proteins or ingested pathological proteins are quickly degraded within microglia (1). In addition, our data did not support the alternative option, that is, that phagocytosis is performed by astrocytes, that can also have scavenger properties under specific conditions (44, 84).

In agreement with little phagocytic activity of glial cells in PD and AD brain, it has been shown that pathological protein

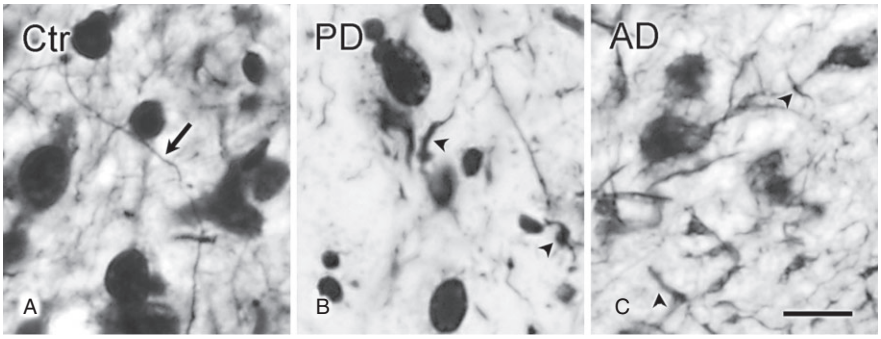

Figure 8. *Bodian staining in the AON of control subjects, PD and AD patients.* **A.** In the AON of control subjects, Bodian staining showed normal appearing neurites (arrow). **B.** In PD patients, and (**C**) in AD patients, Bodian staining showed morphologically altered neurites, and disconnected fiber parts (arrowhead); bar (**A–C**) = 20 μm.

aggregates in an AD mouse model were also surrounded by microglia and astroglia, but were not internalized by these cells (67). In fact, *in vitro* studies suggest that isolated, and healthy, human microglia cells take up Aβ less readily in contrast to peripheral macrophages (20). In addition, macrophages derived from AD patients indeed have poorer Aβ phagocytic properties when compared to macrophages isolated from control subjects (21). Lately, attention has focused on the possibility that the altered morphology of microglial cells during aging or under neurodegenerative conditions is a consequence of microglial senescence rather than a reflection of their activational state (68). Using similar immunohistochemical techniques, the so-called dystrophic microglial cells, rather than "activated" microglial cells, were found to have impaired phagocytic function (69). The concept of dystrophic microglia that develops due to ageing contributes to the idea that microgliosis per se does not cause neuronal death, but acts as a bystander in disease progression, as it may have lost its neuroprotective nature (52, 69).

An alternative explanation for the putative impairment in, or absence of, phagocytic capacity, is that effective phagocytosis by microglial and astroglial cells will depend on the aggregation status of the protein to be eliminated. This would imply that phagocytosis of large aggregated proteins, occurring in progressive or end stage of the disease and probably present in our patient material, is reduced, while truncated or monomeric forms can be cleared (36, 57, 74). This inability of microglia and astrocytes to take appropriate care of pathological protein aggregates (40) would then lead to progressive pathological protein accumulation within the CNS and could induce a feed-forward loop by which further activation of microglia is induced. This may eventually promote more neuronal dysfunction and/or demise.

In summary, we have shown an increase in the density of amoeboid microglia within the AON of the OB, a region beyond the traditional sites of PD and AD neuropathology, occurring irrespective of the type of pathological protein deposited. Correlation analysis between amoeboid microglia density and level of pathological protein deposition within the AON suggests a protein-dependent effect on the amount of activated microglial cells. This is not reflected at the level of phagocytosis since no clear colocalization of pathological proteins with amoeboid microglia or, alternatively, astrocytes was observed. Finally, although a causal relation needs to be proven, we hypothesize that it is not cell loss, but rather an increased density of amoeboid microglial cells, possibly in combination with neurite pathology, that may contribute to the functional deficits in the AON of PD and AD patients, such as hyposmia.

ACKNOWLEDGMENTS

We thank Dr I. Huitinga of the Netherlands Brain Bank for the provision of human post-mortem brain material and Michiel Kooreman for technical support. We gratefully acknowledge the patients and their families for the brain donations. The Stichting Internationaal Parkinson Fonds (IPF; KJD, PJL, A-MvD), and Internationale Stichting Alzheimer Onderzoek (ISAO; KJD, PJL) are kindly acknowledged for financial support.

DISCLOSURE STATEMENT

The authors declare that they have no conflict of interest.

REFERENCES

1. Akiyama H, Schwab C, Kondo H, Mori H, Kametani F, Ikeda K, McGeer PL (1996) Granules in glial cells of patients with Alzheimer's disease are immunopositive for C-terminal sequences of β-amyloid protein. *Neurosci Lett* **206**:169–172.
2. Attems J, Lintner F, Jellinger KA (2005) Olfactory involvement in aging and Alzheimer's disease: an autopsy study. *J Alzheimers Dis* **7**:149–158.
3. Berendse HW, Roos DS, Raijmakers P, Doty RL (2011) Motor and non-motor correlates of olfactory dysfunction in Parkinson's disease. *J Neurol Sci* **310**:21–24.
4. Block ML, Hong JS (2005) Microglia and inflammation-mediated neurodegeneration: multiple triggers with a common mechanism. *Prog Neurobiol* **76**:77–98.
5. Bodian D (1936) A new method for staining nerve fibers and nerve endings in mounted paraffin sections. *Anat Rec* **65**:89–97.
6. Braak H, Braak E (1991) Neuropathological stageing of Alzheimer-related changes. *Acta Neuropathol (Berl)* **82**:239–259.
7. Braak H, Del Tredici K, Bratzke H, Hamm-Clement J, Sandmann-Keil D, Rüb U (2002) Staging of the intracerebral inclusion body pathology associated with idiopathic Parkinson's disease (preclinical and clinical stages). *J Neurol* **249**:1–5.
8. Braak H, Del Tredici K, Rüb U, de Vos RAI, Jansen Steur ENH, Braak E (2003) Staging of brain pathology related to sporadic Parkinson's disease. *Neurobiol Aging* **24**:197–211.
9. Braak H, Ghebremedhin E, Rüb U, Bratzke H, Del Tredici K (2004) Stages in the development of Parkinson's disease-related pathology. *Cell Tissue Res* **318**:121–134.
10. Braak H, Rüb U, Schultz C, Del Tredici K (2006) Vulnerability of cortical neurons to Alzheimer's and Parkinson's diseases. *J Alzheimers Dis* **9**:35–44.
11. Brunjes PC, Illig KR, Meyer EA (2005) A field guide to the anterior olfactory nucleus (cortex). *Brain Res Rev* **50**:305–335.

12. Croisier E, Moran LB, Dexter DT, Pearce RKB, Graeber MB (2005) Microglial inflammation in the parkinsonian substantia nigra: relationship to alpha-synuclein deposition. *J Neuroinflammation* **2**:14–22.
13. Crowther RA (1993) Tau protein and paired helical filaments of Alzheimer's disease. *Curr Opin Struct Biol* **3**:202–206.
14. Curtis MA, Kam M, Nannmark U, Anderson MF, Axell MZ, Wikkelso C *et al* (2007) Human neuroblasts migrate to the olfactory bulb via a lateral ventricular extension. *Science* **315**:1243–1249.
15. Devanand DP, Michaels-Marston KS, Liu X, Pelton GH, Padilla M, Marder K *et al* (2000) Olfactory deficits in patients with mild cognitive impairment predict Alzheimer's disease at follow-up. *Am J Psychiatry* **157**:1399–1405.
16. DiPatre PL, Gelman BB (1997) Microglial cell activation in aging and Alzheimer disease: partial linkage with neurofibrillary tangle burden in the hippocampus. *J Neuropathol Exp Neurol* **56**:143–149.
17. Dodel RC, Lohmüller F, Du Y, Eastwood B, Gocke P, Oertel WH, Gasser T (2001) A polymorphism in the intronic region of the IL-1alpha gene and the risk for Parkinson's disease. *Neurology* **56**:982–983.
18. Doorn KJ, Lucassen PJ, Boddeke HW, Prins M, Berendse HW, Drukarch B, Van Dam AM (2012) Emerging roles of microglial activation and non-motor symptoms in Parkinson's disease. *Prog Neurobiol* **98**:222–238.
19. Doty RL, Hawkes CH, Berendse HW (2011) Olfactory dysfunction in Parkinson's disease and related disorders. In: *Non-Dopamine Lesions in Parkinson's Disease*, GM Halliday, RA Barker, DB Rowe (eds), pp. 65–91. Oxford University Press Inc., New York.
20. Familian A, Eikelenboom P, Veerhuis R (2007) Minocycline does not affect amyloid-β phagocytosis by human microglial cells. *Neurosci Lett* **416**:87–91.
21. Fiala M, Liu PT, Espinosa-Jeffrey A, Rosenthal MJ, Bernard G, Ringman JM *et al* (2007) Innate immunity and transcription of MGAT-III and Toll-like receptors in Alzheimer's disease patients are improved by bisdemethoxycurcumin. *Proc Natl Acad Sci USA* **104**:12849–12854.
22. Gerhard A, Pavese N, Hotton G, Turkheimer F, Es M, Hammers A *et al* (2006) In vivo imaging of microglial activation with [11C](R)-PK11195 PET in idiopathic Parkinson's disease. *Neurobiol Dis* **21**:404–412.
23. Glass CK, Saijo K, Winner B, Marchetto MC, Gage FH (2010) Mechanisms underlying inflammation in neurodegeneration. *Cell* **140**:918–934.
24. Graeber MB, Streit WJ (2010) Microglia: biology and pathology. *Acta Neuropathol (Berl)* **119**:89–105.
25. Gregory GE, Greenway AR, Lord KA (1980) Alcoholic Bouin fixation of insect nervous systems for Bodian silver staining. I,II,III. *Biotechnic & Histochemistry* **55**:143–165.
26. Grimaldi LME, Casadei VM, Ferri C, Veglia F, Licastro F, Annoni G *et al* (2000) Association of early onset Alzheimer's disease with an interleukin(−alpha gene polymorphism. *Ann Neurol* **47**:361–365.
27. Haehner A, Hummel T, Reichmann H (2011) Olfactory loss in Parkinson's disease. *Park Dis* Article ID 450939.
28. Hansen C, Angot E, Bergström AL, Steiner JA, Pieri L, Paul G *et al* (2011) Alpha-synuclein propagates from mouse brain to grafted dopaminergic neurons and seeds aggregation in cultured human cells. *J Clin Invest* **121**:715–725.
29. Hashioka S, Miklossy J, Schwab C, Klegeris A, McGeer PL (2008) Adhesion of exogenous human microglia and THP-1 cells to amyloid plaques of postmortem Alzheimer's disease brain. *J Alzheimers Dis* **14**:345–352.
30. Hirsch EC, Vyas S, Hunot S (2012) Neuroinflammation in Parkinson's disease. *Parkinsonism Relat Disord* **18**:210–212.
31. Hjorth E, Frenkel D, Weiner H, Schultzberg M (2010) Effects of immunomodulatory substances on phagocytosis of $A\beta_{142}$ by human microglia. *International J Alzheimers Dis* Article ID 798424.
32. Holness CL, Simmons DL (1993) Molecular cloning of CD68, a human macrophage marker related to lysosomal glycoproteins. *Blood* **81**:1607–1613.
33. Huisman E, Uylings H, Hoogland PV (2004) A 100% increase of dopaminergic cells in the olfactory bulb may explain hyposmia in Parkinson's disease. *Mov Disord* **19**:687–692.
34. Imamura K, Hishikawa N, Sawada M, Nagatsu T, Yoshida M, Hashizume Y (2003) Distribution of major histocompatibility complex class II-positive microglia and cytokine profile of Parkinson's disease brains. *Acta Neuropathol (Berl)* **106**:518–526.
35. Irwin DJ, White MT, Toledo JB, Xie SX, Robinson JL, Deerlin VV *et al* (2012) Neuropathologic substrates of Parkinson's disease dementia. *Ann Neurol* **72**:587–598.
36. Koenigsknecht J, Landreth G (2004) Microglial phagocytosis of fibrillar β-amyloid through a 1 integrin-dependent mechanism. *J Neurosci* **24**:9838–9846.
37. Kovacs T, Cairns NJ, Lantos PL (1999) beta-amyloid deposition and neurofibrillary tangle formation in the olfactory bulb in ageing and Alzheimer's disease. *Neuropathol Appl Neurobiol* **25**:481–491.
38. Kreutzberg GW (1996) Microglia: a sensor for pathological events in the CNS. *Trends Neurosci* **19**:312–318.
39. Kuhn HG, Palmer TD, Fuchs E (2001) Adult neurogenesis: a compensatory mechanism for neuronal damage. *Eur Arch Psychiatry Clin Neurosci* **251**:152–158.
40. Lai AY, McLaurin JA (2012) Clearance of amyloid-β peptides by microglia and macrophages: the issue of what, when and where. *Future Neurol* **7**:165–176.
41. Lavelle A (1956) Nucleolar and Nissl substance development in nerve cells. *J Comp Neurol* **104**:175–205.
42. Lee HJ, Patel S, Lee SJ (2005) Intravesicular localization and exocytosis of α-synuclein and its aggregates. *J Neurosci* **25**:6016–6024.
43. Lei H, Mooney R, Katz LC (2006) Synaptic integration of olfactory information in mouse anterior olfactory nucleus. *J Neurosci* **26**:12023–12032.
44. Lööv C, Hillered L, Ebendal T, Erlandsson A (2012) Engulfing astrocytes protect neurons from contact-induced apoptosis following injury. *PLoS One* **7**:e33090.
45. Luk KC, Kehm V, Carroll J, Zhang B, O'Brien P, Trojanowski JQ, Lee VMY (2012) Pathological α-synuclein transmission initiates Parkinson-like neurodegeneration in nontransgenic mice. *Science* **338**:949–953.
46. Marlatt MW, Lucassen PJ (2010) Neurogenesis and Alzheimer's disease: biology and pathophysiology in mice and men. *Curr Alzheimer Res* **7**:113–125.
47. McGeer PL, Itagaki S, Boyes BE, McGeer EG (1988) Reactive microglia are positive for HLA−DR in the substantia nigra of Parkinson's and Alzheimer's disease brains. *Neurology* **38**:1285–1286.
48. Mogi M, Harada M, Kondo T, Riederer P, Inagaki H, Minami M, Nagatsu T (1994) Interleukin-1 beta, interleukin-6, epidermal growth factor and transforming growth factor-alpha are elevated in the brain from parkinsonian patients. *Neurosci Lett* **180**:147–150.
49. Mucke L, Selkoe DJ (2012) Neurotoxicity of amyloid β protein: synaptic and network dysfunction. *Cold Spring Harb Perspect Med* 2: a006338.
50. Mundiñano IC, Caballero MC, Ordóñez C, Hernandez M, DiCaudo C, Marcilla I *et al* (2011) Increased dopaminergic cells and protein

aggregates in the olfactory bulb of patients with neurodegenerative disorders. *Acta Neuropathol (Berl)* **122**:61–74.
51. Murphy C, Gilmore MM, Seery CS, Salmon DP, Lasker BR (1990) Olfactory thresholds are associated with degree of dementia in Alzheimer's disease. *Neurobiol Aging* **11**:465–469.
52. Njie MG, Boelen E, Stassen FR, Steinbusch HWM, Borchelt DR, Streit WJ (2010) Ex vivo cultures of microglia from young and aged rodent brain reveal age-related changes in microglial function. *Neurobiol Aging* **33**:195.1–195.12.
53. Oide T, Kinoshita T, Arima K (2006) Regression stage senile plaques in the natural course of Alzheimer's disease. *Neuropathol Appl Neurobiol* **32**:539–556.
54. Ouchi Y, Yagi S, Yokokura M, Sakamoto M (2009) Neuroinflammation in the living brain of Parkinson's disease. *Parkinsonism Relat Disord* **15**:200–204.
55. Overmyer M, Helisalmi S, Soininen H, Laakso M, Riekkinen P Sr, Alafuzoff I (1999) Reactive microglia in aging and dementia: an immunohistochemical study of postmortem human brain tissue. *Acta Neuropathol (Berl)* **97**:383–392.
56. Palop JJ, Chin J, Mucke L (2006) A network dysfunction perspective on neurodegenerative diseases. *Nature* **443**:768–773.
57. Park JY, Paik SR, Jou I, Park SM (2008) Microglial phagocytosis is enhanced by monomeric α-synuclein, not aggregated α-synuclein: implications for Parkinson's disease. *Glia* **56**:1215–1223.
58. Perlmutter LS, Scott SA, Barron E, Chui HC (1992) MHC class II positive microglia in human brain: association with Alzheimer lesions. *J Neurosci Res* **33**:549–558.
59. Pletnikova O, West N, Lee MK, Rudow GL, Skolasky RL, Dawson TM *et al* (2005) Aβ deposition is associated with enhanced cortical α-synuclein lesions in Lewy body diseases. *Neurobiol Aging* **26**:1183–1192.
60. Ponsen MM, Stoffers D, Booij J, van Eck Smit BLF, Wolters EC, Berendse HW (2004) Idiopathic hyposmia as a preclinical sign of Parkinson's disease. *Ann Neurol* **56**:173–181.
61. Price JL (1990) Olfactory system. In: *The Human Nervous System*. G Paxinos, JK Mai (eds.), pp. 979–998. Academic Press: San Diego.
62. Reynolds AD, Glanzer JG, Kadiu I, Ricardo Dukelow M, Chaudhuri A, Ciborowski P *et al* (2008) Nitrated alpha synuclein activated microglial profiling for Parkinson's disease. *J Neurochem* **104**:1504–1525.
63. Saiz-Sanchez D, Ubeda-Banon I, de la Rosa-Prieto C, Argandona-Palacios L, Garcia-Munozguren S, Insausti R, Martinez-Marcos A (2010) Somatostatin, tau, and β-amyloid within the anterior olfactory nucleus in Alzheimer disease. *Exp Neurol* **223**:347–350.
64. Sasaki A, Kawarabayashi T, Murakami T, Matsubara E, Ikeda M, Hagiwara H *et al* (2008) Microglial activation in brain lesions with tau deposits: comparison of human tauopathies and tau transgenic mice TgTauP301L. *Brain Res* **1214**:159–168.
65. Selkoe DJ (1991) The molecular pathology of Alzheimer's disease. *Neuron* **6**:487–498.
66. Spillantini MG, Crowther RA, Jakes R, Hasegawa M, Goedert M (1998) Alpha-synuclein in filamentous inclusions of Lewy bodies from Parkinson's disease and dementia with Lewy bodies. *Proc Natl Acad Sci USA* **95**:6469–6473.
67. Stalder M, Deller T, Staufenbiel M, Jucker M (2001) 3D-Reconstruction of microglia and amyloid in APP23 transgenic mice: no evidence of intracellular amyloid. *Neurobiol Aging* **22**:427–434.
68. Streit WJ, Sammons NW, Kuhns AJ, Sparks DL (2004) Dystrophic microglia in the aging human brain. *Glia* **45**:208–212.
69. Streit WJ, Braak H, Xue QS, Bechmann I (2009) Dystrophic (senescent) rather than activated microglial cells are associated with tau pathology and likely precede neurodegeneration in Alzheimer's disease. *Acta Neuropathol (Berl)* **118**:475–485.
70. Strohmeyer R, Kovelowski C, Mastroeni D, Leonard B, Grover A, Rogers J (2005) Microglial responses to amyloid β peptide opsonization and indomethacin treatment. *J Neuroinflammation* **2**:18–29.
71. Su X, Maguire-Zeiss KA, Giuliano R, Prifti L, Venkatesh K, Federoff HJ (2008) Synuclein activates microglia in a model of Parkinson's disease. *Neurobiol Aging* **29**:1690–1701.
72. Su X, Federoff HJ, Maguire-Zeiss KA (2009) Mutant alpha-synuclein overexpression mediates early proinflammatory activity. *Neurotox Res* **16**:238–254.
73. Tan J, Town T, Paris D, Mori T, Suo Z, Crawford F *et al* (1999) Microglial activation resulting from CD40-CD40L interaction after β-amyloid stimulation. *Science* **286**:2352–2355.
74. Thal DR, Schultz C, Dehghani F, Yamaguchi H, Braak H, Braak E (2000) Amyloid β-protein (A+β)-containing astrocytes are located preferentially near N-terminal-truncated A+β deposits in the human entorhinal cortex. *Acta Neuropathol (Berl)* **100**:608–617.
75. Tsuboi Y, Wszolek ZK, Graff-Radford NR, Cookson N, Dickson DW (2003) Tau pathology in the olfactory bulb correlates with Braak stage, Lewy body pathology and apolipoprotein ε4. *Neuropathol Appl Neurobiol* **29**:503–510.
76. van den Berge SA, van Strien ME, Korecka JA, Dijkstra AA, Sluijs JA, Kooijman L *et al* (2011) The proliferative capacity of the subventricular zone is maintained in the parkinsonian brain. *Brain* **134**:3249–3263.
77. Van Everbroeck B, Dobbeleir I, De Waele M, De Leenheir E, Lübke U, Martin JJ, Cras P (2004) Extracellular protein deposition correlates with glial activation and oxidative stress in Creutzfeldt-Jakob and Alzheimer's disease. *Acta Neuropathol (Berl)* **108**:194–200.
78. Versijpt JJ, Dumont F, Van Laere KJ, Decoo D, Santens P, Audenaert K *et al* (2003) Assessment of neuroinflammation and microglial activation in Alzheimer's disease with radiolabelled PK11195 and single photon emission computed tomography. *Eur Neurol* **50**:39–47.
79. Vilhardt F (2005) Microglia: phagocyte and glia cell. *Int J Biochem Cell Biol* **37**:17–21.
80. Vroon A, Drukarch B, Bol JGJM, Cras P, Brevé JJP, Allan SM *et al* (2007) Neuroinflammation in Parkinson's patients and MPTP-treated mice is not restricted to the nigrostriatal system: microgliosis and differential expression of interleukin-1 receptors in the olfactory bulb. *Exp Gerontol* **42**:762–771.
81. Walter L, Neumann H (2009) Role of microglia in neuronal degeneration and regeneration. *Semin Immunopathol* **31**:513–525.
82. Watson MB, Richter F, Lee SK, Gabby L, Wu J, Masliah E *et al* (2012) Regionally-specific microglial activation in young mice over-expressing human wildtype alpha-synuclein. *Exp Neurol* **237**:318–334.
83. West MJ, Slomianka L, Gundersen HJG (1991) Unbiased stereological estimation of the total number of neurons in the subdivisions of the rat hippocampus using the optical fractionator. *Anat Rec* **231**:482–497.
84. Wyss-Coray T, Loike JD, Brionne TC, Lu E, Anankov R, Yan F *et al* (2003) Adult mouse astrocytes degrade amyloid-β in vitro and in situ. *Nat Med* **9**:453–457.
85. Zhang W, Wang T, Pei Z, Miller DS, Wu X, Block ML *et al* (2005) Aggregated alpha-synuclein activates microglia: a process leading to disease progression in Parkinson's disease. *FASEB J* **19**:533–542.